


 Cite this: *RSC Adv.*, 2024, **14**, 17710

## Exploration of novel cationic amino acid-enriched short peptides: design, SPPS, biological evaluation and *in silico* study†

Prashant K. Chandole,<sup>a</sup> Tushar Janardan Pawar,<sup>b</sup> José Luis Olivares-Romero,<sup>b</sup> Sunil R. Tivari,<sup>a</sup> Bianney Garcia Lara,<sup>c</sup> Harun Patel,<sup>d</sup> Iqrar Ahmad,<sup>d</sup> Enrique Delgado-Alvarado,<sup>b</sup> Siddhant V. Kokate<sup>\*f</sup> and Yashwantsinh Jadeja<sup>b</sup><sup>\*</sup>

Antimicrobial resistance (AMR) represents a critical challenge worldwide, necessitating the pursuit of novel approaches to counteract bacterial and fungal pathogens. In this context, we explored the potential of cationic amino acid-enriched short peptides, synthesized via solid-phase methods, as innovative antimicrobial candidates. Our comprehensive evaluation assessed the antibacterial and antifungal efficacy of these peptides against a panel of significant pathogens, including *Escherichia coli*, *Pseudomonas aeruginosa*, *Staphylococcus aureus*, *Streptococcus pyogenes*, *Candida albicans*, and *Aspergillus niger*. Utilizing molecular docking techniques, we delved into the molecular interactions underpinning the peptides' action against these microorganisms. The results revealed a spectrum of inhibitory activities, with certain peptide sequences displaying pronounced effectiveness across various pathogens. These findings underscore the peptides' potential as promising antimicrobial agents, with molecular docking offering valuable insights into their mechanisms of action. This study enriches antimicrobial peptide (AMP) research by identifying promising candidates for further refinement and development toward therapeutic application, highlighting their significance in addressing the urgent issue of AMR.

Received 5th December 2023

Accepted 28th May 2024

DOI: 10.1039/d3ra08313f

[rsc.li/rsc-advances](http://rsc.li/rsc-advances)

## Introduction

The escalating challenge of antimicrobial resistance (AMR) has become a critical concern for global health, necessitating innovative and multifaceted strategies to combat bacterial and fungal infections.<sup>1</sup> As traditional antibiotics increasingly fall short against multidrug-resistant pathogens, the scientific community is urgently seeking innovative approaches to address this crisis.<sup>2</sup> In this context, the development of short peptides, particularly those enriched with cationic amino acids,

has emerged as a promising avenue for novel antimicrobial agents.<sup>3</sup> Antimicrobial Peptides (AMPs) represent an essential class of molecules within the innate immune defences of various organisms, including humans, plants, and insects.<sup>4</sup> Characterized by their broad-spectrum activity against bacteria, fungi, viruses, and certain parasites, AMPs offer a versatile approach to combating infections. Their effectiveness is primarily attributed to their ability to disrupt microbial membranes, leading to cell lysis and pathogen death.<sup>5</sup>

Among AMPs, short cationic amino acid-enriched peptides have drawn significant attention due to their potent antimicrobial properties and lower risk of resistance development.<sup>6</sup> The foundation of their potency is firmly anchored in their cationic residues that bestow a positive charge upon these peptides.<sup>6</sup> This pivotal characteristic instigates a symphony of electrostatic interactions with microbial cell membranes adorned with negative charges, thereby triggering a nuanced molecular dialogue.<sup>6c</sup> As the peptides engage in binding, a transformative narrative unfolds, underscored by the disruption of membrane integrity, propelling a cascade of events culminating in the demise of microorganisms.<sup>6d,e</sup> Beyond their immediate disruptive potential, the positive charge holds the promise of selectivity, with intriguing indications that certain short cationic peptides exhibit a predilection for microbial cells over their mammalian counterparts.<sup>7</sup> This intricate mode of

<sup>a</sup>Department of Chemistry, Marwadi University, Rajkot-360003, Gujarat, India.  
E-mail: drysjadeja@gmail.com

<sup>b</sup>Red de Estudios Moleculares Avanzados, Instituto de Ecología, A.C. Carretera Antigua a Coatepec 351, Xalapa, 91073, Veracruz, Mexico

<sup>c</sup>Departamento de Química, Universidad de Guanajuato, Noria Alta S/N, Guanajuato-36050, Guanajuato, Mexico

<sup>d</sup>Department of Pharmaceutical Chemistry, R. C. Patel Institute of Pharmaceutical Education and Research, Shirpur District Dhule-425405, Maharashtra, India

<sup>e</sup>Micro and Nanotechnology Research Center, Universidad Veracruzana, Blvd. Av. Ruiz Cortines No. 455 Fracc. Costa Verde, Boca del Río 94294, Mexico

<sup>f</sup>Department of Chemistry, S. S. C. College, Junnar, Pune-410502, Maharashtra, India.  
E-mail: siddhantkokate@gmail.com

† Electronic supplementary information (ESI) available: The spectral data of the study is provided. It includes <sup>1</sup>H and <sup>13</sup>C NMR, and mass spectral data. See DOI: <https://doi.org/10.1039/d3ra08313f>



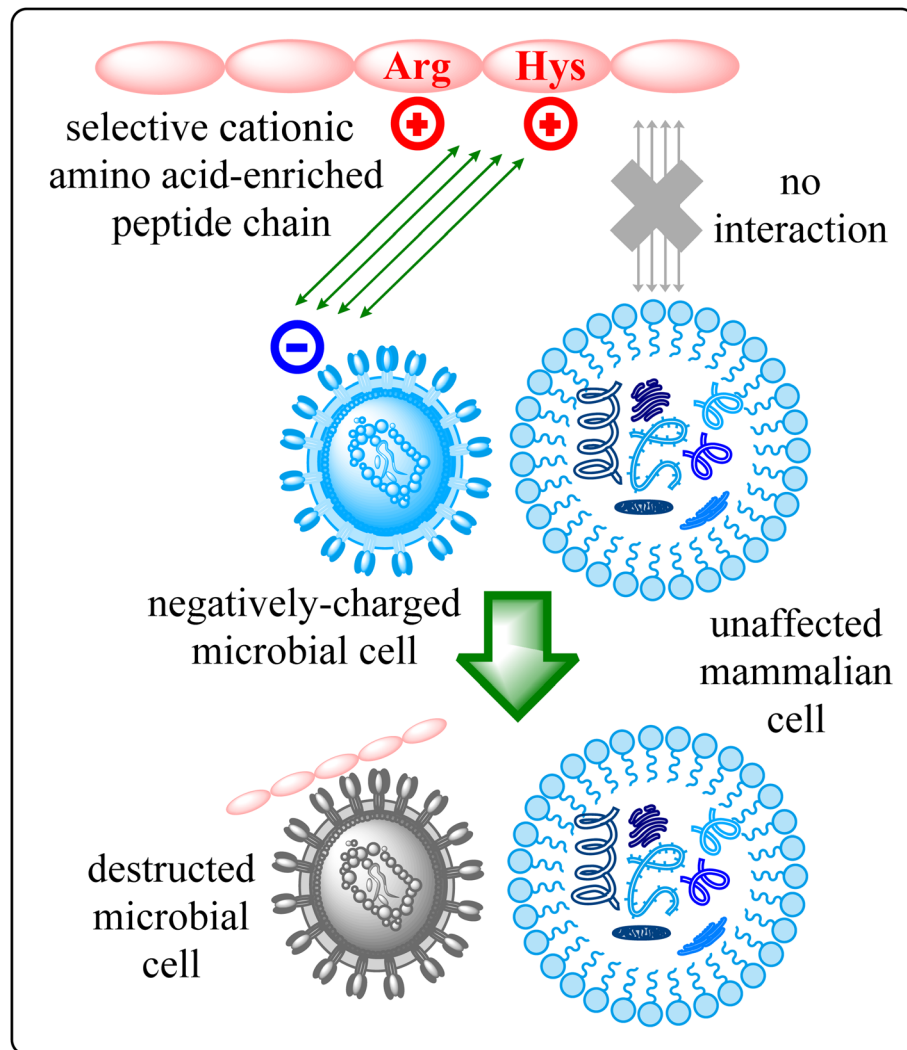


Fig. 1 Schematic representation of short cationic amino acid-enriched peptide mode of action.

action is visually encapsulated in Fig. 1, where the schematic representation elucidates the journey of these short cationic AA-enriched peptides—from their initial electrostatic interaction to the culmination of the microorganism's downfall. This figure serves as a beacon, illuminating the mechanistic essence that underpins the potential of these peptides to revolutionize the landscape of antimicrobial strategies.

The smaller size and higher solubility of short cationic AA-enriched peptides compared to monoclonal antibodies provide better pharmacokinetics, higher cellular uptake in the target tissue, and rapid clearance from the non-target tissues.<sup>8</sup> Such peptides that are effectively taken up by cells are called Cell Penetrating Peptides (CPPs).<sup>9</sup> Such short cationic AA-enriched peptides are a group of small peptides consisting of 2–30 AAs that can pass the lipid bilayer of cells without disturbing their structural and functional integrity and carry bioactive molecules, like nucleic acids,<sup>10</sup> proteins,<sup>11</sup> bioimaging agents<sup>12</sup> or nanoparticles<sup>13</sup> across the cell membrane. Thus, they are also known as protein transduction domains (PTDs). They are primarily small cationic peptides, histidine (His),<sup>14</sup> arginine

(Arg)<sup>15</sup> or lysine (Lys)<sup>16</sup> rich peptides. The His-rich CPPs are particularly utilized for the transduction of small interfering RNA (siRNA) or DNA derivatives inside cells.<sup>17</sup> In contrast, Arg-rich CPPs have the capability of efficient internalization and deliver biologically active cargoes.<sup>18</sup>

In recent years, the exploration of short peptides has grown due to their inherent advantages over traditional antibiotics.<sup>19</sup> Their adaptability for synthesis and modification, facilitated by established techniques like solid-phase peptide synthesis (SPPS),<sup>20</sup> positions them as a platform for innovative antimicrobial design. Against this backdrop, the current study embarks on an expedition into the design, synthesis, and comprehensive evaluation of cationic AA-enriched short peptides. Rigorous and careful assessments encompass antibacterial and antifungal activities, encompassing a spectrum of clinically relevant strains. This is synergistically complemented by molecular docking analyses, which penetrate the subtleties of peptide-microbe interactions and furnish insights to guide rational design strategies. Recent studies employing molecular docking and simulation have shed light on the structural

determinants of peptide efficacy and offered guidelines for the rational design of new antimicrobial candidates.<sup>19,21</sup>

Remarkably, the strength of such cationic AA-enriched short peptides can be further bolstered by their cystine-containing composition—a structural feature that imparts robust stability and endows them with the resilience to thwart enzymatic degradation.<sup>22</sup> Moreover, Cys residue can provide a site for the conjugation of the peptide to another molecule *via* the  $-\text{SH}$  group. Additionally, N-terminal Cys improves the helical propensity of the molecule along with its cell penetration power, which in turn aids to improve its biological activity. Furthermore, hydrophobic AAs consisting non-polar side chains, like Leu, Val, Ala, Ile, Gly, Pro, *etc.* can increase the hydrophobicity and helical content of peptides, which in turn can increase their biological activity.<sup>23</sup> It has been very well explored that the higher overall hydrophobicity of peptides could favour their penetration into the lipid bilayer of the cell membrane.<sup>24</sup> Considering this, we have designed **7a–e** which consists hydrophobic AAs with non-polar side chains, *viz.*, Gly (**7a**), Ala (**7b**), Val (**7c**), Leu (**7d**), and Pro (**7e**). The hydrophobicity of each derivative will be calculated and it is anticipated that higher the hydrophobicity higher is the biological activity of the peptide derivative. Additionally, AAs with polar and hydrophobic side chains, like Ser, Thr, Tyr, Asn, and Gln enable peptide derivatives to have an amphipathic character which is a really important feature for peptide therapeutics to exhibit significant biological activities.<sup>25</sup> Thus, in this study, we have designed one derivative, **7f**, consisting Tyr which has a polar side chain with the anticipation of showing good biological activity.

In this study, we investigate the potential of such cationic AA-enriched short peptides as potent antimicrobial agents. Solid-phase peptide synthesis (SPPS) technology further supports the development of these peptides by enabling precise control over their composition and structure. This study builds upon the foundation of molecular docking insights and SPPS advancements to design, synthesize, and evaluate a new series of cationic amino acid-enriched short peptides. Through a comprehensive set of antibacterial and antifungal assays, coupled with detailed molecular docking simulations, we explore the interactions between these peptides and various pathogens, including *Escherichia coli*, *Pseudomonas aeruginosa*, *Staphylococcus aureus*, *Streptococcus pyogenes*, *Candida albicans*, and *Aspergillus niger*.

## Material and methods

The 2-chlorotriyl chloride (2-CTC) resin was employed for the synthesis of a series of Cys rich cationic AA-enriched short peptides. Highly efficient loading estimation is obtained from using such resin. This resin is mainly used for the synthesis of short-chain peptides.<sup>26</sup> It was purchased from Merck. Fmoc(9-fluorenylmethoxycarbonyl)-protected L-amino acids were utilized and acquired from Sichuan, China. HBTU (2-(1H-benzotriazol-1-yl)-1,1,3,3-tetramethyluronium) and triisopropylsilane (TIS) were acquired from survival chemical. HOBr·H<sub>2</sub>O (*N*-hydroxybenzotriazole monohydrate),

diisopropylethylamine (DIPEA) and trifluoroacetic acid (TFA) acquired from spectrochem. Phenol acquired from SD fine chemicals. A fully automated CSBio peptide synthesizer (CS136X) was utilized for the synthesis of derivatives.<sup>21</sup>

An open capillary method was utilized to determine the melting points which were uncorrected. The Kaiser test was used for monitoring the deprotection and coupling reactions. A mixture of ethyl acetate and *n*-hexanes was used for the purification of the derivatives. Shimadzu liquid chromatography mass spectrometry (LC-MS) (at 70 eV) mass spectrometer (ESI) was used to determine the mass spectra. Bruker Avance 400 MHz NMR (nuclear magnetic resonance) spectrometer was used to determine the <sup>1</sup>H and <sup>13</sup>C NMR spectra using DMSO-*d*<sub>6</sub> (deuterated dimethyl sulfoxide) solvent.<sup>21</sup>

## Experimental section

### Synthetic route for the formation of intermediate Fmoc-Cys(Trt)-CT resin 1

The 2-CTC resin was introduced to the peptide synthesizer with a substitution of 1.0 mmol g<sup>-1</sup>. The resin was initially rinsed with dichloromethane (DCM; 10 volumes) and then drained. After that, DCM (10 volumes) was added, and the reaction mass was stirred for 60 minutes for swelling before being drained. Following this, Fmoc-Cys(Trt)-OH (3.0 equiv.) was dissolved in DCM (8 volumes) and transferred into the reaction vessel. DIPEA (6 equiv.) was subsequently added to the reaction vessel and stirred at 28 °C for 2 hours. The peptidyl resin was filtered after the 2 hours mark and washed twice with DCM and once with dimethylformamide (DMF).<sup>27</sup> A solution containing DIPEA, methanol (MeOH), and DCM (1:2:7) was used to cap the unreacted functional groups of the resin. The loading percentage was monitored using an ultraviolet (UV) spectrophotometer.<sup>21</sup>

### Synthetic route for the formation of intermediates 6a–f

The Standard Fmoc protocol was employed to produce the desired intermediates **6a–f** through the Solid Phase Peptide Synthesis (SPPS) method. In the SPPS reaction vessel, the Fmoc-Cys(Trt)-CT resin was swollen in 20 volumes of DMF for thirty minutes. The CSBio peptide synthesizer facilitated the synthesis of the intended intermediates. Post-swelling, the following steps were repeated for the synthesis of the intermediates: (a) deprotection of the Fmoc group was carried out using 20% piperidine/DMF (v/v) (10 v). The resin was washed twice (5 minutes and 10 minutes each). The Kaiser test was used to ensure complete deprotection, indicated by the appearance of a blue colour test solution and resin beads. Subsequently, the reaction mass (peptidyl resin) was filtered and washed thrice with DMF, once with iso-propyl alcohol (IPA), and thrice again with DMF. (b) For all the coupling reactions, Fmoc AA (3.0 equiv., 3 mmol concerning initial resin loading), HBTU (3.0 equiv., 3 mmol), HOBr·H<sub>2</sub>O (3.0 equiv., 3 mmol), and DIPEA (6.0 equiv., 6 mmol) in 8 volumes of DMF were utilized. All the coupling reactions required one hour of stirring. The Kaiser test was used to confirm the completion of the reaction, indicated



by a colourless test solution and resin beads. The reaction mass (peptidyl resin) was then filtered and washed five times with DMF to yield fmoc-protected intermediates.<sup>28</sup> Additionally, fmoc group deprotection was carried out using 20% piperidine/DMF (v/v) (10 v) to obtain the desired intermediates **6a–i**. The Kaiser test was used to confirm the deprotection of the Fmoc group, where blue colour resin beads and test solution were observed, confirming the completion of the step. Following this, the reaction mass (peptidyl resin) was filtered and washed five times with DMF to produce **6a–i**.<sup>21</sup>

#### Synthetic route for the synthesis of desired cationic AA-enriched short peptides **7a–f**

A cleavage cocktail consisting of a mixture of TIS : H<sub>2</sub>O : TFA (10 : 10 : 80) (10 mL g<sup>-1</sup>) was utilized for the cleavage of the sidechain and CTC resin.<sup>29</sup> The protected peptidyl resin was stirred in the cleavage cocktail for 3 hours at 27 ± 2 °C. After 3 h, the reaction mass was filtered, and the filtrate obtained was precipitated using chilled diisopropyl ether (DIPE) (50 v). Subsequently, the reaction mass was stirred at 0–5 °C for 2 hours, filtered, and washed thrice with chilled DIPE (10 v). Finally, the wet cake was dried at 30 °C under vacuum to yield the desired products.<sup>21</sup>

## Results and discussion

### Chemistry

In response to the escalating challenge of antimicrobial resistance, our study embarked on the synthesis of a novel series of cationic short peptides, enriched with cysteine and denoted as compounds **7a–f**. Utilizing solid-phase peptide synthesis (SPPS) with the HBTU/HOBt coupling protocol, we successfully synthesized these peptides in a stable, powdered form (Scheme 1).

The synthesis commenced with the synthesis of Fmoc-Cys(Trt)-2-CT resin **1**. This was achieved by attaching Fmoc-Cys(Trt)-OH to the 2-CTC resin, utilizing DIPEA and DCM as the solvent. Following this, the Fmoc protective group was removed from compound **1** using a 20% solution of piperidine in DMF. This deprotection step yielded the H-Cys(Trt)-2-CT resin **2**, revealing the free amino (-NH<sub>2</sub>) group at its N-terminus. The successful removal of the Fmoc group was confirmed by a positive Kaiser test, indicated by the transformation of the test solution and resin to a dark blue color. After the initial deprotection, Fmoc-Arg(Pbf)-OH was coupled to compound **2** under conditions facilitated by HBTU/HOBt, leading to the formation of Fmoc-Arg(Pbf)-Cys(Trt)-2-CT resin **3**. The completion of this coupling reaction was verified through the Kaiser test, with a colorless test solution and resin beads indicating completion of the reaction. Further removal of the Fmoc group from compound **3** resulted in the formation of H-Arg(Pbf)-Cys(Trt)-2-CT resin **4**.

Continuing the synthesis, *in situ* coupling of the compound **4** with the next set of amino acids (AAs)—namely histidine, proline, and an additional cysteine—was conducted under the established HBTU/HOBt conditions, followed by the

deprotection of the Fmoc group. This iterative process yielded the H-Cys(Trt)-Pro-His(Trt)-Arg(Pbf)-Cys(Trt)-2-CT resin intermediates **5**. Subsequently, six different protected amino acids (Fmoc-R(SPG)-OH) were incorporated using the same HBTU/HOBt conditions, with subsequent deprotection of the Fmoc group. This sequence of actions produced the H-R(SPG)-Cys(Trt)-Pro-His(Trt)-Arg(Pbf)-Cys(Trt)-2-CT resin intermediates **6a–f**.

The culmination of the synthesis was marked by global cleavage, performed over three hours at room temperature with a cleavage cocktail of TIS : H<sub>2</sub>O : TFA in a 10 : 10 : 80 ratio. This step precipitated the desired short peptides through DIPE, effectively separating them from the CTC resin and side-product groups (SPGs). This step is also known as “acidolysis.” Purification using ethyl acetate and *n*-hexane refined the crude product, resulting in the isolation of compounds **7a–f** with yields ranging from 78% to 89%.

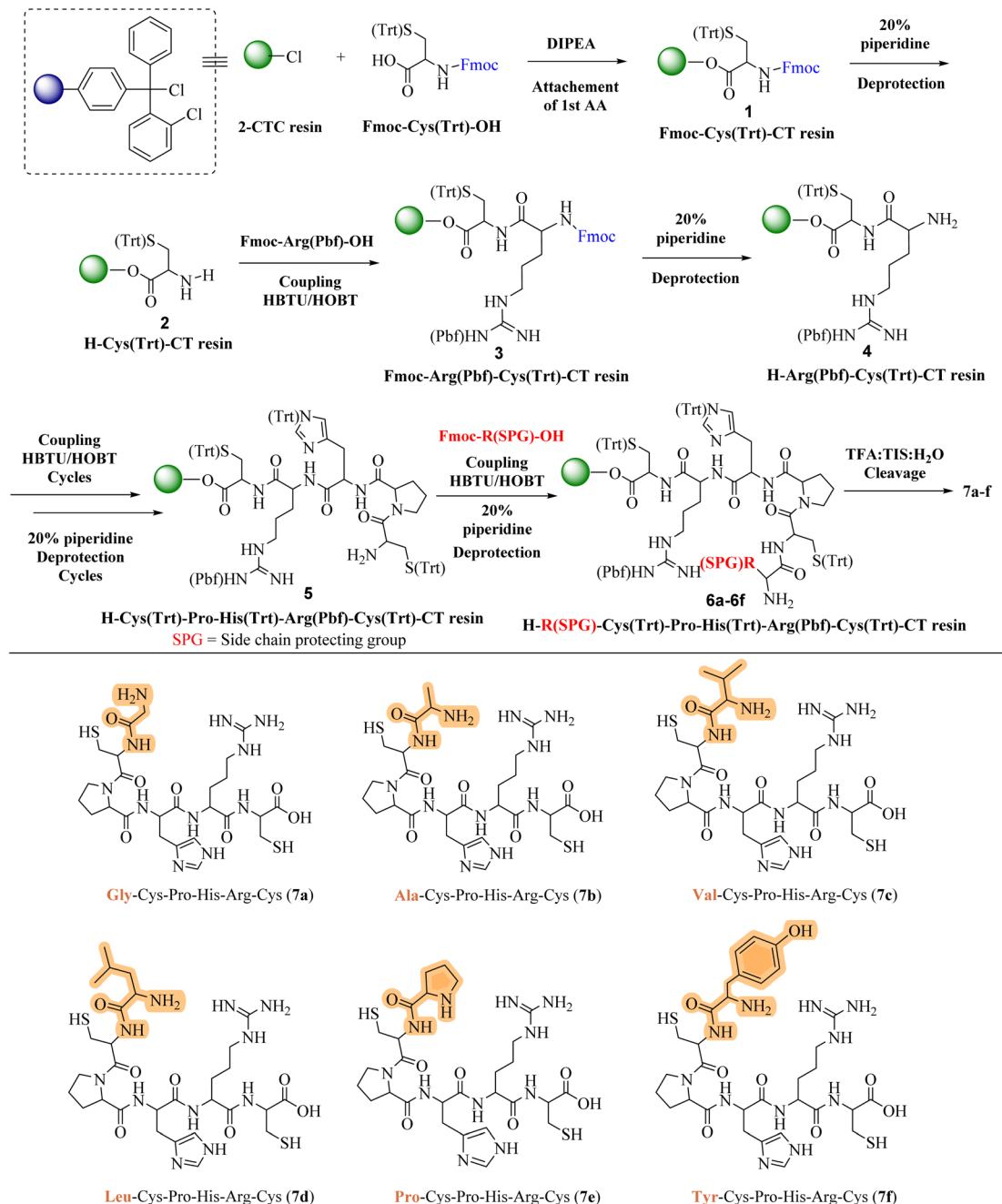
Each peptide, depicted in Scheme 1, underwent thorough characterization *via* <sup>1</sup>H, <sup>13</sup>C NMR (ESI<sup>†</sup>), and mass spectral analysis, affirming the integrity of their structures. The series encompassed peptides with varied AA substitutions—Gly in **7a**, Ala in **7b**, Val in **7c**, Leu in **7d**, Pro in **7e**, and Tyr in **7f**—to explore and compare their antimicrobial activities. The inclusion of different Fmoc-protected AAs and SPGs at strategic synthesis points introduced a diversity of structural features crucial for a comprehensive biological evaluation.

### Docking study

*Candida albicans*, commonly known as *C. albicans*, exists as a commensal organism, coexisting harmoniously as part of the natural human microflora in approximately 50% of the population.<sup>30</sup> While yeast is generally benign in individuals with robust health, it has the potential to transform into a pathogen, instigating life-threatening infections in those who are immunocompromised or debilitated. The proteolytic activity stands out as a crucial virulence factor associated with *C. albicans*. This proteolytic activity is linked to the secreted aspartic proteinases (Saps) of *C. albicans*, comprising a minimum of 10 distinct members. Sap1–8 are released into the extracellular space, while Sap 9–10 manifest as glycosylphosphatidylinositol (GPI)-anchored membrane-bound proteins. Several studies have substantiated the significance of Sap5 in contributing to virulence during both local and systemic infections caused by *C. albicans*.<sup>31</sup>

Docking protocol was cross-validated by redocking a ligand back into its binding site in the protein structure to compare the predicted binding pose with the experimentally observed pose. Both, co-crystallized ligand and docked ligand were having RMSD value of 1.82 Å. The docking study of the cationic amino acid-enriched short peptides towards the aspartic proteinase (Sap 5) from *C. albicans* revealed that short peptides formed multiple interactions with the Sap 5 enzyme (Fig. 2 and 3). Peptide **7e** showed the highest docking score of the -10.198 kcal mol<sup>-1</sup> towards the Sap 5 enzyme. It formed 09 hydrogen bond interactions with the 07 amino acids of Sap 5 enzyme, namely Asp 218, Thr 221, Thr 222, Arg 299, Glu 300, Gly





**Scheme 1** Solid-phased peptide synthesis of cationic amino acid-enriched short peptides 7a–f.

85, and Asp 86. Compound 7d, which was found to be a potent compound of the series against the *in vitro* assay against the *C. albicans*, was having a docking score of  $-8.52$  kcal mol $^{-1}$  and showed interaction with the 07 amino acids *via* the hydrogen bonding as shown in Table 1. This interaction includes the following amino acid residues: Glu 132, Asp 303, Lys 83, Gly 85, Asp 86, Gly 220, and Lys 192 (Fig. 2).<sup>32</sup>

### MD simulation result

Molecular dynamic simulation (MDS) is a powerful tool for studying ligand binding, protein folding, and conformational

changes.<sup>33</sup> It can reveal the positions of all the atoms at femtosecond temporal resolution and provide accurate estimates of ligand binding affinities. The MD simulation was performed for 200 ns to gain insights into the conformational changes that occur in the Sap 5 enzyme when compound 7d binds into the pocket of the enzyme. A single file of compound 7d in complex with Sap 5 enzyme was saved in the pdb file format and later subjected to the 200 ns time of simulation.

To conduct an MDS, a system was constructed using the SPC solvent model. The SPC model is a widely used explicit solvent model that employs a combination of interactions, such as van



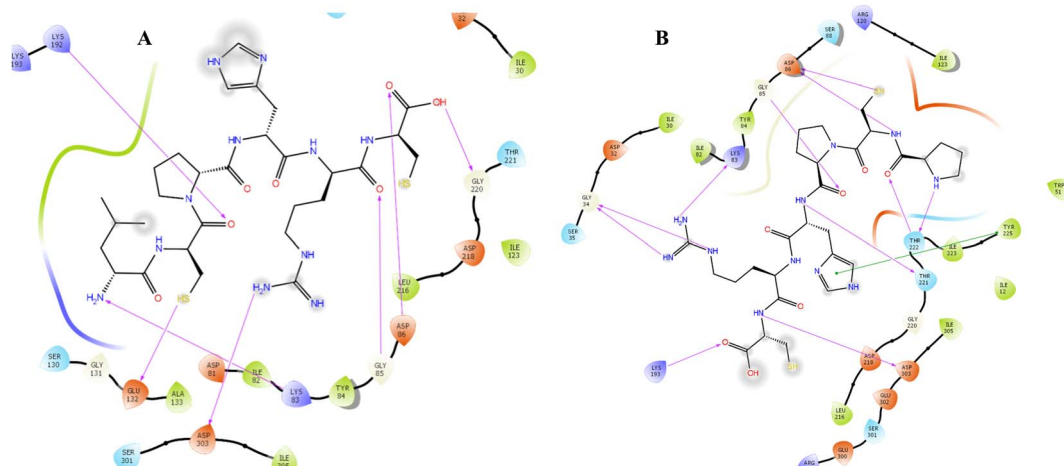


Fig. 2 Docking interaction of compound 7d (A) and 7e (B) with the aspartic proteinase (Sap 5) from *C. albicans*.

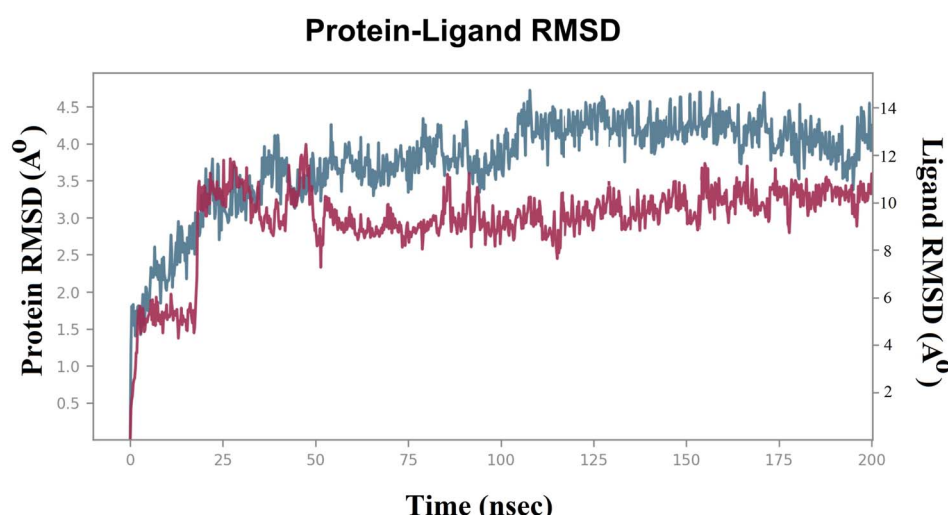


Fig. 3 RMSD of the compound 7d and Sap 5 enzyme in bound form.

der Waals and electrostatic forces, to represent the behavior of solvent molecule.<sup>34</sup> The system was set up with an orthorhombic boundary condition and a box size of  $5 \times 5 \times 5$  Å. This boundary condition is a type of periodic boundary condition that closely resembles a cubic cell in use. To achieve system neutralization, counter ions (13 Na<sup>+</sup> and 18 Cl<sup>-</sup>) were introduced. This process is essential to balance the system's overall charge, particularly in the presence of a charged biomolecular system, ensuring that the electrostatic energy is accurately calculated during the simulation.<sup>35</sup> The system was then prepared for the 200 ns production phase of the MDS through a series of minimization and equilibration steps under NPT conditions. After the minimization process, a 200 ns MDS was performed to investigate the conformational stability and changes of the complex involving Sap 5 and compound 7d.

To evaluate the stability of the system during the MDS, parameters such as the “root mean square deviation (RMSD)” and “root mean square fluctuation (RMSF)” were calculated for

both the Sap 5 enzyme and compound 7d.<sup>36,37</sup> The RMSD measures the deviation of the protein structure from its initial conformation, while the RMSF measures the fluctuation of each atom in the protein over time.<sup>22,23</sup> These parameters are commonly used to assess the stability of the system during the simulation and to identify regions of the protein that undergo

Table 1 Docking score of the cationic amino acid-enriched short peptides towards the aspartic proteinase (Sap 5) from *C. albicans*

Title	Docking score (kcal mol <sup>-1</sup> )	Glide emodel	Glide energy
7e	-10.198	-122.438	-79.703
7d	-8.52	-119.225	-82.513
7a	-8.344	-112.734	-85.848
7b	-8.197	-120.133	-78.636
7c	-8.045	-104.461	-69.745
7f	-6.771	-94.334	-72.8



significant conformational changes upon ligand binding.<sup>22,23</sup> Lower RMSD values indicate a more stable system.<sup>22,23</sup> In the case of the compound **7d**-Sap 5 complex, the ligand's RMSD initially exhibited fluctuations ranging from 4.5 Å to 6.0 Å (net RMSD 1.5 Å) during the first 5 ns, primarily due to equilibration (Fig. 3). The fluctuations in ligand RMSD observed around the 25 ns were likely due to the flexibility of the peptide (Fig. 3). From 50 ns to 200 ns, the RMSD of the compound **7d**-Sap 5 complex remained relatively constant, fluctuating between 8.5 Å and 10.5 Å (net RMSD 2.0 Å) (Fig. 3).

RMSF, or root mean square fluctuation, serves as an indicator of protein structure flexibility, which is crucial for assessing system stability during MDS.<sup>22,23</sup> It measures the fluctuations in backbone and ligand atoms throughout the 200 ns MDS of the compound **7d**-Sap 5 complex. This analysis provides insights into the dynamic behavior of the complex, allowing for the assessment of its stability and the identification of conformational changes over the course of the simulation.<sup>22,23</sup> The analysis in Fig. 4 indicates that there were no significant fluctuations in the amino acid residues upon the binding of compound **7d** to the active site of Sap 5. This suggests that the binding of compound **7d** did not induce substantial conformational changes in the protein structure, and the complex remained relatively stable throughout the simulation. The RMSF values for the protein's backbone residues within the catalytic domain ranged from 0.5 Å to 1.8 Å (Fig. 4). Slightly higher fluctuations were observed around the 50 residue index and 80–90 residue index, where the RMSF reached 3 Å. Compound **7d** interacted with 42 amino acids of the Sap 5, including Ala-11, Thr-13, Val-29, Asp-32, Gly-34, Ser-35, Lys-50, Trp-51, Asp-81, Lys-83, Tyr-84, Gly-85, Asp-86, Gly-87, Ser-88, Tyr-89, Thr-117, Ala-119, Arg-120, Lys-121, Ile-12, Ser-130, Gly-131, Glu-132, Lys-192, Lys-193, Leu-216, Asp-218, Ser-219, Gly-220, Thr-221, Thr-222, Tyr-225, Asn-249, Lys-257,

Thr-258, Ile-298, Ser-301, Gly-302, Asp-303, Ile-305 and Glu-335 (Fig. 4). The RMSF values for all of these interacting residues were below 1.8 Å, except for Lys-50, Trp-51, Asp-81, Lys-83, Tyr-84, Gly-85, Asp-86, Gly-87, Ser-88, and Tyr-89, which exhibited an RMSF from 2.8–3.2 Å, as indicated by the green vertical bars as shown in Fig. 4.

We conducted a detailed analysis of the interaction between compound **7d** and Sap 5 throughout the 200 ns simulation (Fig. 5). This analysis aimed to provide insights into the dynamic behaviour of the complex and the specific regions that contribute most to its flexibility during the simulation. The Sap 5 enzyme exhibited multiple interactions with compound **7d**, with the most significant interaction observed between the Gly-85, Ser-88, and Lys-50 residues and the peptide backbone of compound **7d**. The imidazole ring of compound **7d** formed a hydrogen bond interaction with the Asp-218 residue of Sap-5 (Fig. 5). We have also measured the radius of gyration of the compound **7d** during 200 ns time of simulation. Radius of gyration indicates the overall fluctuation of ligand and on an average, it was found to be 0.8 Å (5.6 to 6.4 Å) (Fig. 5).

### Docking and MD simulation procedure

The Glide SP docking molecular docking tool of Schrödinger Inc., USA was employed for molecular docking study. Protein preparation was conducted using the 'protein preparation wizard' within Maestro 8.0 to optimize the protein structure of Sap 5 enzyme (2QZX) using the OPLS 2005 force field. The grid was meticulously prepared by centering the ligand within the crystal structure using default box dimensions. The ligands were built using the "build panel of LigPrep 2.2" module, which generates the low energy conformer employing the OPLS 2005 force field. The low-energy conformers were meticulously docked into the generated grid using the standard precision (SP) method.<sup>32</sup>

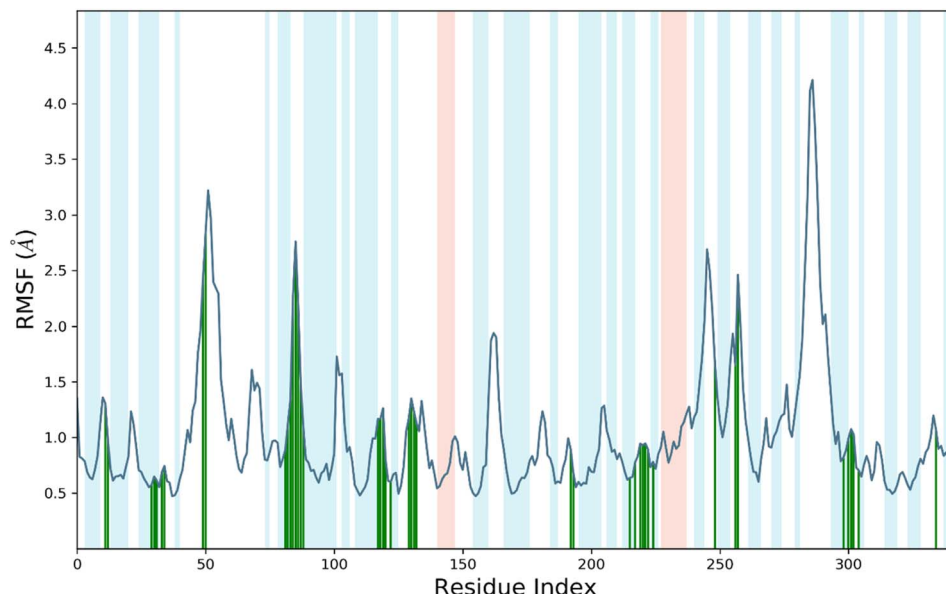


Fig. 4 RMSF of Sap 5 enzyme during 200 ns time of simulation.



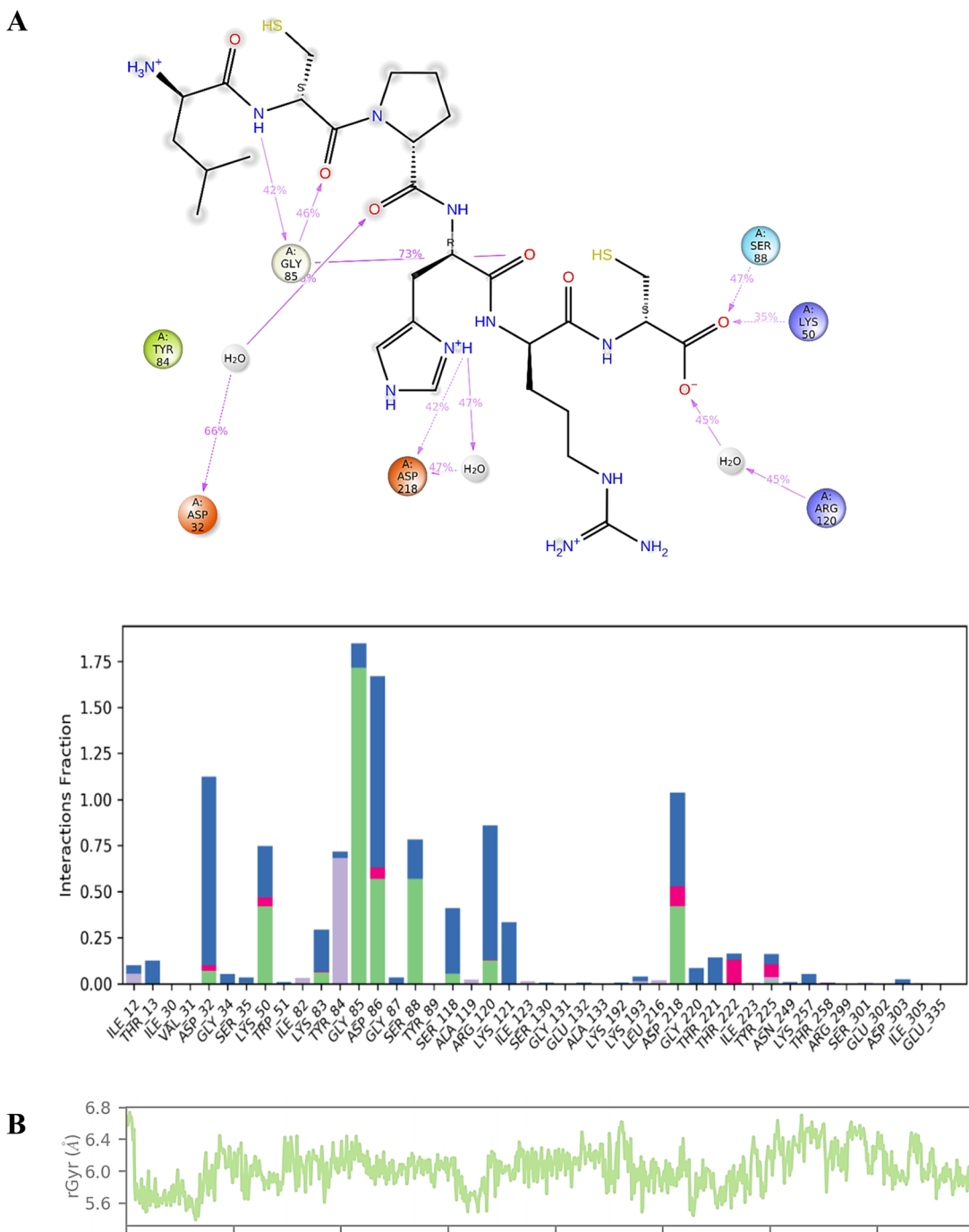


Fig. 5 (A) Interaction profile of the compound **7d** with Sap 5 enzyme during 200 ns time of simulation; (B) radius of gyration of compound **7d** during 200 ns time of simulation.

To conduct MDS, a solitary file containing the compound **7d** in complex with the Sap5 enzyme was saved in the pdb file format. Subsequently, it underwent a 200 ns simulation period using the SPC solvent model. The system was set up with an orthorhombic boundary condition and a box size of  $5 \times 5 \times 5 \text{ \AA}$ . The system was neutralized by 13  $\text{Na}^+$  and 18  $\text{Cl}^-$  counter ions. The system was then prepared for the 200 ns production phase of the MDS through a series of minimization and equilibration steps under NPT conditions. After the minimization process,

a 200 ns MDS was performed to investigate the conformational stability and changes of the ligand–receptor complex.<sup>33–37</sup>

## Determination of peptide hydrophobicity

The hydrophobicity values of designed cationic AA enriched short peptide **7a-f** were theoretically calculated using the relevant equations. The Eisenberg method<sup>38</sup> was used to calculate the mean hydrophobicity value for each cationic AA enriched short peptide by employing the following eqn (1):

$$\langle H \rangle = \left( \sum_{i=1}^n H_i \right) / N \quad (1)$$

where  $\langle H \rangle$  is the mean hydrophobicity of the peptide sequence,  $H_i$  is the hydrophobicity of the  $i$ th AA in the peptide sequence and  $N$  is the number of AA residues. The values of hydrophobicity for each AA were based on the hydrophobicity scale by Fauchère and Pliska which uses the octanol–water partition coefficients.<sup>39</sup>

As mentioned earlier in the article, higher overall hydrophobicity of peptides could favour their penetration into the lipid bilayer of the cell membrane and thus increase their biological activity. As shown in Table 2, theoretically, compound **7d** showed the highest mean hydrophobicity value of 0.77 among all synthesized cationic AA enriched short peptides **7a–f** and is expected to show the highest biological activity. Whereas, theoretically, peptide derivative **7a** showed the least mean hydrophobicity value of 0.49 (Fig. 6) and is expected to show the least biological activity among all the peptide derivatives. It is well known fact that higher the  $\langle H \rangle$  value, greater is the hydrophobicity of the peptide sequence.

### Biological evaluation

The microorganisms, including *Escherichia coli* MTCC 443, *Pseudomonas aeruginosa* MTCC 1688, *Streptococcus pyogenes* MTCC 442, *Staphylococcus aureus* MTCC 96, *Aspergillus niger* MTCC 282, and *Candida albicans* MTCC 227, were obtained from King Abdullah University Hospital (KAUH), Irbid, Jordan. They were stored at  $-70^{\circ}\text{C}$  in trypticase-soy broth with 20% glycerol from BBL Microbiology Systems (Cockeysville, Md, USA) until required for batch susceptibility testing. To ensure purity and viability, the organisms were thawed and subcultured three times. The *in vitro* antimicrobial activities of the synthesized compounds **7a–f** were studied using the conventional Mueller Hinton Broth-microdilution method.<sup>40</sup> This method is used for quantitative antimicrobial susceptibility testing and to determine the minimum inhibitory concentration (MIC) of antimicrobial agents. The test involved screening microorganisms for visible growth in broth, consisting of different dilutions of the antimicrobial agents. The MIC value indicates the lowest concentration of an antimicrobial agent that inhibits visible growth within a specified time frame. The microbroth dilution method offers several advantages over the macrobroth dilution method, including miniaturization and automation through the use of disposable small plastic “microdilution” trays. Its practicality and popularity in research are attributed to advantages such as reproducibility, prepared

Table 2 The mean hydrophobicity of synthesized derivatives **7a–f**

Compound	<b>7a</b>	<b>7b</b>	<b>7c</b>	<b>7d</b>	<b>7e</b>	<b>7f</b>
$\langle H \rangle^a$	0.49	0.54	0.69	0.77	0.61	0.65

<sup>a</sup>  $\langle H \rangle$  is the mean hydrophobicity of the peptide sequence.

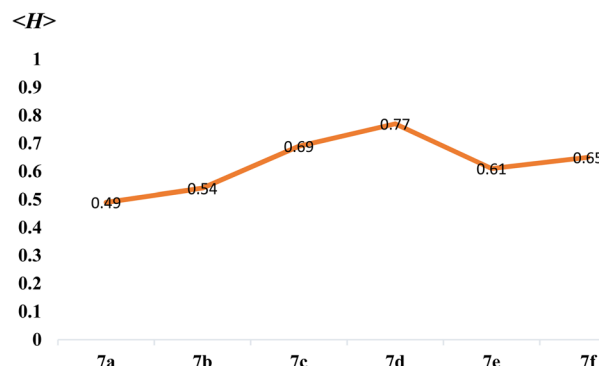


Fig. 6 The graphical demonstration of mean hydrophobicity of peptide derivatives **7a–f**.

panels, cost-effective reagents, and space optimization resulting from its miniaturization.<sup>41,42</sup>

### The procedure for antibacterial activity assay

The strains employed in the study were recently acquired and stored under optimal conditions. The compounds underwent screening for their antibacterial activity in triplicate experiments against the bacteria, employing different concentrations of 1000, 500, 250, and 200  $\mu\text{g mL}^{-1}$  substances exhibiting effective inhibition were subsequently subjected to dilution and further testing. The antibacterial assay employed the Mueller Hinton Broth dilution method. A suspension of the respective bacteria at a concentration of 10  $\mu\text{g mL}^{-1}$  was inoculated on suitable media, and growth was monitored following incubation at  $37^{\circ}\text{C}$  for one to two days. The test mixture was intended to contain  $10^8$  cells per mL. Ampicillin served as the standard drug for assessing antibacterial activity in this study.<sup>40</sup>

### The procedure for antifungal activity assay

The strains employed in this study were recently acquired and appropriately stored. The substances underwent screening for their anti-fungal properties in triplicate experiments against the fungi at varying concentrations of 1000, 500, 250, and 200  $\mu\text{g mL}^{-1}$ . The active compounds were further diluted and subjected to additional testing. The antifungal assay utilized the Muller Hinton Broth dilution method. Fungal growth was monitored using Sabouraud's dextrose broth at  $28^{\circ}\text{C}$  under aerobic conditions for a period of 48 hours. Nystatin served as the standard for comparative analysis.<sup>40</sup>

The antibacterial activities of novel cationic AA enriched short peptide conjugate **7a–f** against all bacterial strains are shown in Table 3. The cationic peptide conjugate **7d** containing Leu was found to be 4 times more potent against *E. coli* and showed an excellent activity with the highest MIC value of 25  $\mu\text{g mL}^{-1}$  among all the synthesized peptide conjugates as compared with the standard drug Ampicillin which had a MIC of 100  $\mu\text{g mL}^{-1}$  against the same bacterial strain *E. coli* (Fig. 7). The compound **7c** with Val showed an excellent activity with MIC value of 40  $\mu\text{g mL}^{-1}$ , 2.5 times more potency against *E. coli* as compared with standard Ampicillin. The cationic peptide



**Table 3** Antibacterial and antifungal activities of the synthesized derivatives **7a–f**<sup>a</sup>

Compound	MIC (anti-bacterial activity) in $\mu\text{g mL}^{-1}$				MIC (anti-fungal activity) in $\mu\text{g mL}^{-1}$	
	<i>E. c.</i>	<i>P. a.</i>	<i>S. a.</i>	<i>S. p.</i>	<i>C. a.</i>	<i>A. n.</i>
<b>7a</b>	80	90	200	90	60	65
<b>7b</b>	45	50	125	80	55	50
<b>7c</b>	40	50	110	45	35	40
<b>7d</b>	25	40	90	20	20	35
<b>7e</b>	50	70	125	60	50	55
<b>7f</b>	45	50	110	55	40	50
Ampicillin	100	100	250	100	—	—
Nystatin	—	—	—	—	100	100

<sup>a</sup> *E. c.*: *Escherichia coli*, *P. a.*: *Pseudomonas aeruginosa*, *S. a.*: *Staphylococcus aureus*, *S. p.*: *Streptococcus pyogenes*, *C. a.*: *Candida albicans*, *A. n.*: *Aspergillus niger*.

conjugates **7b**, **7e**, and **7f** also exhibited good activities with MIC values (in  $\mu\text{g mL}^{-1}$ ) of 45, 50 and 45, respectively, and were around 2 times more potent than the control drug. Against *P. aeruginosa*, **7d** exhibited the highest activity among all the peptide derivatives with MIC value of  $40 \mu\text{g mL}^{-1}$ , 2.5 times more potency as compared with the standard drug Ampicillin which had a MIC of  $100 \mu\text{g mL}^{-1}$  against the same. Moreover, compounds **7b**, **7c** and **7f** also exhibited good activity with MIC values of  $50 \mu\text{g mL}^{-1}$  and were 2 times more potent than the control drug. Furthermore, among all the synthesized cationic AA enriched short peptides, **7d** showed the best antibacterial activity against *Staphylococcus aureus* with MIC value of  $90 \mu\text{g mL}^{-1}$  as compared to the standard drug Ampicillin ( $250 \mu\text{g mL}^{-1}$ ). The other peptide derivatives, **7b**, **7c**, **7e**, and **7f**, were almost twice potent as the control drug against *Staphylococcus aureus* with MIC values (in  $\mu\text{g mL}^{-1}$ ) of 125, 110, 125, and 110, respectively. For the activity against *Streptococcus pyogenes*, the derivative **7d** showed an excellent activity with a MIC value of  $20 \mu\text{g mL}^{-1}$  and was five time more potent as compared with a standard drug which had a MIC of  $100 \mu\text{g mL}^{-1}$ . The

compound **7c** also showed good activity with MIC value of  $45 \mu\text{g mL}^{-1}$ , 2 times more potency as compared with standard Ampicillin, whereas derivatives **7b**, **7e** and **7f** exhibited moderate activities (MIC of 80, 60 and  $55 \mu\text{g mL}^{-1}$ , respectively) as compared to the control drug.

From the antibacterial study data of peptide derivatives **7a–f** against all four bacterial strains, it was seen that the peptide conjugate **7a** showed almost same activities as the standard drug Ampicillin and was least active among all the synthesized derivatives, whereas the peptide derivative **7d** was the most potent among them. Cationic AA enriched short peptides containing hydrophobic AAs which has non-polar sidechains, composed mostly of carbon and hydrogen, like Leu, Val, Ala, Pro, are known for their excellent cell-penetrating ability and biological activities.<sup>43–45</sup> This is well supported by the theoretical calculations of the mean hydrophobicity of synthesized peptides **7a–f** (Table 2), in which derivative **7d** exhibited the highest mean hydrophobicity value of 0.77 and was expected to be the most potent among all the synthesized peptides, whereas the peptide derivative **7a** showed the lowest mean hydrophobicity value of 0.49 and was expected to show the least potency against all bacterial strains. Similar to compound **7d**, compounds **7c** and **7f** showed higher mean hydrophobicity 0.69 and 0.65, respectively, due to the presence of higher number of hydrocarbons in their side chains and thus, showed better cell penetrating ability and in turn showed better antibacterial activity as compared to **7a**, **7b** and **7e**, which has lesser number of hydrocarbons in their sidechains and thus, their ability to penetrate cell membrane is weaker, which explains their weaker activity against bacterial strains.

The antifungal activities of cationic AA enriched short peptide conjugates **7a–f** against all the fungal strains are shown in Table 3. Against *Candida albicans*, the peptide conjugate **7d** was the most active with an excellent MIC value of  $20 \mu\text{g mL}^{-1}$  and was five times more potent as compared to Nystatin which was active at  $100 \mu\text{g mL}^{-1}$  (Fig. 8). Peptide conjugates **7c**, **7e**, and **7f** also exhibited good activities against *Candida albicans* with MIC values of 35, 50 and  $40 \mu\text{g mL}^{-1}$ , respectively. Moreover, peptide derivatives **7a** and **7b** showed moderate activities with MIC values of 60 and  $55 \mu\text{g mL}^{-1}$ , respectively, as compared to the standard drug Nystatin. Against the second fungal strain

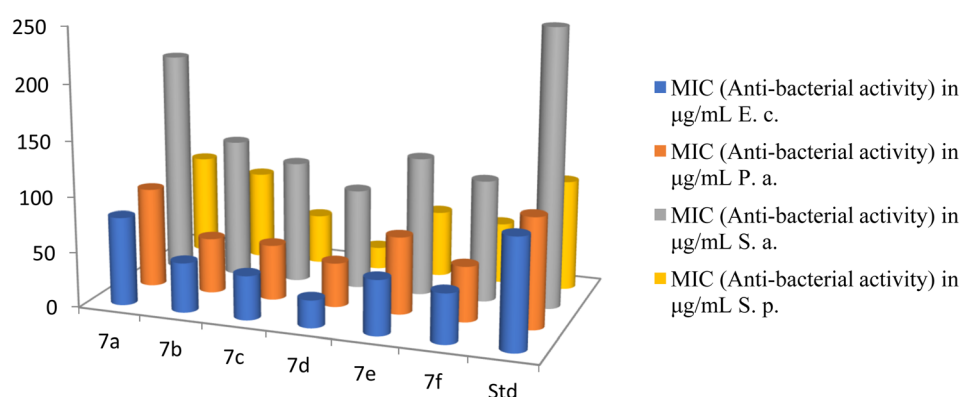


Fig. 7 The antibacterial activities of the synthesized peptides **7a–f**.



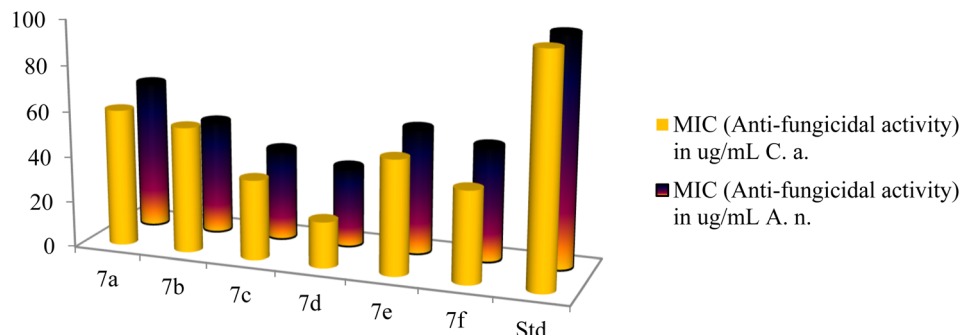


Fig. 8 The antibacterial activities of the synthesized peptides 7a–f.

*Aspergillus niger*, the peptide conjugate **7d** was the most potent with MIC value of  $35 \mu\text{g mL}^{-1}$  and was almost three times more potent as compared to Nystatin which was active at  $100 \mu\text{g mL}^{-1}$ . Compounds **7b**, **7c** and **7f** also displayed good inhibition against *Aspergillus niger* with a MIC value of 50, 40 and  $50 \mu\text{g mL}^{-1}$ , respectively, as compared to the control drug. However, synthesized derivatives **7a** and **7e** showed moderate activities with MIC values of 65 and  $55 \mu\text{g mL}^{-1}$  against *Aspergillus niger*.

From the antifungal study results of peptide derivatives **7a–f** against both fungal strains, it was seen that the peptide conjugate **7a** was least active among all the synthesized derivatives, whereas the peptide derivative **7d** was the most potent among them. For this aspect, the antifungal study results showed the same trend as the antibacterial study. The antifungal study results support the theoretical prediction draw by the hydrophobicity data of all cationic AA enriched short peptide derivatives, where **7d** was expected to be the most potent against both fungal strains among all the synthesized peptides due the highest mean hydrophobicity value of 0.77, whereas the peptide derivative **7a** showed the least potency against both fungal strains due to the lowest mean hydrophobicity value of 0.49. Similar to compound **7d**, compounds **7c** and **7f** showed higher mean hydrophobicity 0.69 and 0.65, respectively, due to the presence of higher number of hydrocarbons in their side chains and thus, showed better cell penetrating ability and in turn showed better antifungal activity as compared to **7a**, **7b** and **7e**, which has lesser number of hydrocarbons in their sidechains and thus, their ability to penetrate cell membrane is weaker, which explains their weaker activity against fungal strains.

## Conclusions

In conclusion, our research underscores the significant potential of cationic amino acid-enriched short peptides in combating antimicrobial resistance, leveraging solid-phase peptide synthesis for its adaptability and scalability. Extensive biological evaluations against key clinical pathogens have unveiled a spectrum of antimicrobial activity, highlighting sequences with outstanding inhibitory effectiveness. Analyses of peptide hydrophobicity have offered crucial insights, clarifying the role of hydrophobic amino acids in enhancing

antimicrobial efficacy. Furthermore, molecular docking studies have provided essential mechanistic understanding, connecting empirical outcomes to theoretical perspectives and underscoring the impact of structural attributes on peptide functionality. As we advance in the antimicrobial research domain, these peptides emerge as innovative assets with broad implications for medicinal chemistry and microbiology. In the face of growing antibiotic resistance challenges, this study contributes vital insights and opens new pathways for the development of effective antimicrobial strategies, positioning cationic amino acid-enriched short peptides as pivotal in reshaping future infection control and therapeutic approaches, and igniting renewed hope for more efficacious antimicrobial interventions.

## Author contributions

All the authors are responsible for the following: study conception and design, data collection, analysis, interpretation of results and manuscript preparation. All the authors reviewed the results and approved the final version of the manuscript.

## Conflicts of interest

The authors declare no conflicts of interest regarding the publication of this paper.

## Acknowledgements

The authors thank University Grants Commission, New Delhi, and Marwadi University, for technical and academic support. Also, TJP acknowledges CONAHCyT for a postdoctoral fellowship (I1200/320/2022-MOD.ORD./09/2022). We are grateful to Dr Juan Luis Monribot-Villanueva for his expertise in HRMS-QTOF analysis.

## References

- For selected reviews on antimicrobial resistance, see: (a) P. Butaye, E. V. Duijkeren, J. Prescott and S. Schwarz, Antimicrobial resistance in bacteria from animals and the environment, *Vet. Microbiol.*, 2014, **171**, 269–272; (b) R. Patini, G. Mangino, L. Martellacci, G. Quaranta,



L. Masucci and P. Gallenzi, The Effect of Different Antibiotic Regimens on Bacterial Resistance: A Systematic Review, *Antibiotics*, 2020, **9**, 22; (c) R. Urban-Chmiel, A. Marek, D. Stępień-Pyśniak, K. Wieczorek, M. Dec, A. Nowaczek and J. Osek, Antibiotic Resistance in Bacteria-A Review, *Antibiotics*, 2022, **11**, 1079; (d) M. Chatzopoulou and L. Reynolds, The Role of Antimicrobial Restrictions in Bacterial Resistance Control: A Systematic Literature Review, *J. Hosp. Infect.*, 2020, **104**, 125–136.

2 (a) R. M. V. Harten, R. Willems, N. Martin and A. Hendrickx, Multidrug-Resistant Enterococcal Infections: New Compounds, Novel Antimicrobial Therapies?, *Trends Microbiol.*, 2017, **25**, 467–479; (b) G. Cheng, M. Dai, S. Ahmed, H. Hao, X. Wang and Z. Yuan, Antimicrobial Drugs in Fighting against Antimicrobial Resistance, *Front. Microbiol.*, 2016, **7**, 470; (c) E. Kamali, A. Jamali, A. Ardebili, F. Ezadi and A. Mohebbi, Evaluation of antimicrobial resistance, biofilm forming potential, and the presence of biofilm-related genes among clinical isolates of *Pseudomonas aeruginosa*, *BMC Res. Notes*, 2020, **13**, 27.

3 For selected reviews on short peptides and their antimicrobial activities, see: (a) N. H. Ishak and N. M. Sarbon, A Review of Protein Hydrolysates and Bioactive Peptides Deriving from Wastes Generated by Fish Processing, *Food Bioprocess Technol.*, 2017, **11**, 2–16; (b) W. Zhang, Y. Zhang, R. Wang, P. Zhang, Y. Zhang, E. Randell, M. Zhang and Q. Jia, A review: Development and application of surface molecularly imprinted polymers toward amino acids, peptides, and proteins, *Anal. Chim. Acta*, 2022, **1234**, 340319; (c) S. Yang, M. Wang, T. Wang, M. Sun, H. Huang, X. Shi, S. Duan, Y. Wu, J. Zhu and F. Liu, Self-assembled short peptides: Recent advances and strategies for potential pharmaceutical applications, *Mater. Today Bio*, 2023, **20**, 100644; (d) X. Hu, M. Liao, H. Gong, L. Zhang, H. Cox, T. A. Waigh and J. R. Lu, Recent advances in short peptide self-assembly: from rational design to novel applications, *Curr. Opin. Colloid Interface Sci.*, 2020, **45**, 1–13; (e) R. Perlikowska, Whether short peptides are good candidates for future neuroprotective therapeutics?, *Peptides*, 2021, **140**, 170528.

4 For selected reviews on antimicrobial peptides (AMP's), see: (a) H. Luong, T. T. Thanh and T. H. Tran, Antimicrobial peptides – Advances in development of therapeutic applications, *Life Sci.*, 2020, **260**, 118407; (b) B. Bechinger and S. Gorr, Antimicrobial Peptides: Mechanisms of Action and Resistance, *J. Dent. Res.*, 2017, **96**, 254–260; (c) D. Fry, Antimicrobial Peptides, *Surg. Infect.*, 2018, **19**, 804–811; (d) D. K. Govindarajan and K. Kandaswamy, Antimicrobial peptides: A small molecule for sustainable healthcare applications. *Medicine in Microecology*, 2023, 100090 (e) K. Nogrado, P. Adisakwattana and O. Reamtong, Antimicrobial peptides: On future antiprotozoal and anthelminthic applications, *Acta Trop.*, 2022, **235**, 106665.

5 For selected articles on mode of action of antimicrobial peptides, see: (a) S. Li, Y. Wang, Z. Xue, Y. Jia, R. Li, C. He and H. Chen, The structure-mechanism relationship and mode of actions of antimicrobial peptides: A review, *Trends Food Sci. Technol.*, 2021, **109**, 103–115; (b) J. E. Nielsen, V. A. Bjørnestad, V. Pipich, H. Jenssen and R. Lund, Beyond structural models for the mode of action: How natural antimicrobial peptides affect lipid transport, *J. Colloid Interface Sci.*, 2021, **582**, 793–802; (c) M. Wenzel, P. Schriek, P. Prochnow, H. B. Albada, N. Metzler-Nolte and J. E. Bandow, Influence of lipidation on the mode of action of a small RW-rich antimicrobial peptide, *Biochim. Biophys. Acta, Biomembr.*, 2016, **1858**, 1004–1011.

6 For selected reviews on cationic peptides, see: (a) U. L. Urmí, A. K. Vijay, R. Kuppusamy, S. Islam and M. D. P. Willcox, A review of the antiviral activity of cationic antimicrobial peptides, *Peptides*, 2023, **166**, 171024; (b) M. I. Sajid, M. Moazzam, R. Stueber, S. E. Park, Y. Cho, N. U. A. Malik and R. K. Tiwari, Applications of amphipathic and cationic cyclic cell-penetrating peptides: Significant therapeutic delivery tool, *Peptides*, 2021, **141**, 170542; (c) A. Vedadghavami, C. Zhang and A. G. Bajpayee, *Nanotoday*, 2020, **34**, 100898; (d) D. Ciumac, H. Gong, X. Hu and J. R. Lu, Membrane targeting cationic antimicrobial peptides, *J. Colloid Interface Sci.*, 2019, **537**, 163–185; (e) S. Matamouros, S. I. Miller and S. Typhimurium, strategies to resist killing by cationic antimicrobial peptides, *Biochim. Biophys. Acta, Biomembr.*, 2015, **1848**, 3021–3025.

7 (a) R. González-Castro, M. Gómez-Lim and F. Plisson, Cysteine-Rich Peptides: Hyperstable Scaffolds for Protein Engineering, *ChemBioChem*, 2020, **22**, 961–973; (b) C. Navo, A. Asín, E. Gómez-Orte, M. Gutiérrez-Jiménez, I. Compañón, B. Ezcurra, A. Avenoza, J. Bustos, F. Corzana, M. Zurbano, G. Jiménez-Osés, J. Cabello and J. Peregrina, Cell-Penetrating Peptides Containing Fluorescent D-Cysteines, *Chemistry*, 2018, **24**, 7991–8000.

8 D. Wu, Y. Gao, Y. Qi, L. Chen, Y. Ma and Y. Li, *Cancer Lett.*, 2014, **351**(1), 13–22.

9 S. R. MacEwan and A. Chilkoti, *Wiley Interdiscip. Rev.: Nanomed. Nanobiotechnol.*, 2013, **5**(1), 31–48.

10 E. Belnoue, A. A. Leystra, S. Carboni, H. S. Cooper, R. T. Macedo, K. N. Harvey, K. N. Colby, K. S. Campbell, L. A. Vanderveer, M. L. Clapper and M. Derouazi, *Cancer*, 2021, **13**(4), 845.

11 M. Lichtenstein, S. Zabit, N. Hauser, S. Farouz, O. Melloul, J. Hirbawi and H. Lorberboum-Galski, *Life*, 2021, **11**(9), 924.

12 E. Kondo, H. Iioka and K. Saito, *Cancer Sci.*, 2021, **112**, 2118–2121.

13 Y. Wang, C.-H. Liu, T. Ji, M. Mehta, W. Wang, E. Marino, J. Chen and D. S. Kohane, *Nat. Commun.*, 2019, **10**(1), 804.

14 S. Alizadeh, S. Irani, A. Bolhassani, S. M. Sadat and J. Avicenna, *Med. Biotechnol.*, 2020, **12**(1), 8.

15 S. Futaki, T. Suzuki, W. Ohashi, T. Yagami, S. Tanaka, K. Ueda and Y. Sugiura, *J. Biol. Chem.*, 2001, **276**(8), 5836–5840.

16 J. C. Mai, H. Shen, S. C. Watkins, T. Cheng and P. D. Robbins, *J. Biol. Chem.*, 2002, **277**(33), 30208–30218.

17 L. Porosk, P. Arukuusk, K. Pöhako, K. Kurrikoff, K. Kiisholts, K. Padari, M. Pooga and U. Langel, *Biomater. Sci.*, 2019, **7**(10), 4363–4374.



18 G. Tünemann, G. Ter-Avetisyan, R. M. Martin, M. Stöckl, A. Herrmann and M. C. Cardoso, *J. Pept. Sci.*, 2008, **14**(4), 469–476.

19 (a) V. Apostolopoulos, J. Bojarska, T. Chai, S. Elnagdy, K. Kaczmarek, J. Matsoukas, R. New, K. Parang, O. Lopez, H. Parhiz, C. Perera, M. Pickholz, M. Remko, M. Saviano, M. Skwarczynski, Y. Tang, W. Wolf, T. Yoshiya, J. Zabrocki, P. Zielenkiewicz, M. AlKhazindar, V. Barriga, K. Kelaidonis, E. Sarasia and I. Toth, A Global Review on Short Peptides: Frontiers and Perspectives, *Molecules*, 2021, **26**, 430; (b) A. Cerrato, S. Aita, A. Capriotti, C. Cavaliere, C. Montone, A. Lagana and S. Piovesana, A new opening for the tricky untargeted investigation of natural and modified short peptides, *Talanta*, 2020, **219**, 121262; (c) S. R. Tivari, S. V. Kokate, U. B. Shelar and Y. Jadeja, The design, synthesis and biological evaluation of the peptide derivatives containing guanidine moiety with 5-chlorothiophene-2-carboxylic acid conjugates, *Rasayan J. Chem.*, 2022, **15**, 875–884; (d) S. R. Tivari, S. V. Kokate, M. S. Gayke, I. Ahmad, H. Patel, S. G. Kumar and Y. Jadeja, A Series of Dipeptide Derivatives Containing (S)-5-Oxopyrrolidine-2-carboxylic acid Conjugates: Design, Solid-Phase Peptide Synthesis, *in vitro* Biological Evaluation, and Molecular Docking Studies, *ChemistrySelect*, 2022, **7**, e202203462; (e) S. R. Tivari, S. V. Kokate, E. M. Sobhia, S. G. Kumar, U. B. Shelar and Y. Jadeja, A Series of Novel Bioactive Cyclic Peptides: Synthesis by Head-to-Tail Cyclization Approach, Antimicrobial Activity and Molecular Docking Studies, *ChemistrySelect*, 2022, **7**, e202201481.

20 H. Yan and F.-E. Chen, Recent Progress in Solid-Phase Total Synthesis of Naturally Occurring Small Peptides, *Adv. Synth. Catal.*, 2022, **364**, 1934–1961.

21 S. R. Tivari, S. V. Kokate, E. Delgado-Alvarado, M. S. Gayke, A. Kotmale, H. Patel, I. Ahmad, E. M. Sobhia, S. G. Kumar, B. G. Lara, V. D. Jain and Y. Jadeja, A novel series of dipeptide derivatives containing indole-3-carboxylic acid conjugates as potential antimicrobial agents: the design, solid phase peptide synthesis, *in vitro* biological evaluation, and molecular docking study, *RSC Adv.*, 2023, **13**, 24250–24263.

22 C. T. Walsh, Tailoring enzyme strategies and functional groups in biosynthetic pathways, *Nat. Prod. Rep.*, 2023, **40**, 326–386.

23 C. Chen, J. Hu, S. Zhang, P. Zhou, X. Zhao, H. Xu, X. Zhao, M. Yaseen and J. R. Lu, *Biomaterials*, 2012, **33**(2), 592–603.

24 K.-Y. Huang, Y.-J. Tseng, H.-J. Kao, C.-H. Chen, H.-H. Yang and S.-L. Weng, *Sci. Rep.*, 2021, **11**, 13594.

25 (a) A. Elliott, J. Huang, S. Neve, J. Zuegg, I. Edwards, A. Cain, C. Boinett, L. Barquist, C. Lundberg, J. Steen, M. Butler, M. Mobli, K. Porter, M. Blaskovich, S. Lociuro, M. Strandh and M. Cooper, *Nat. Commun.*, 2020, **11**, 3184; (b) F. Qiu, Y. Chen, C. Tang and X. Zhao, *Int. J. Nanomed.*, 2018, **13**, 5003–5022.

26 D. M. M. Jaradat, Thirteen decades of peptide synthesis: key developments in solid phase peptide synthesis and amide bond formation utilized in peptide ligation, *Amino Acids*, 2017, **50**, 39–68.

27 V. Made, S. Els-Heindl and A. Beck-Sickinger, Automated solid-phase peptide synthesis to obtain therapeutic peptides, *Beilstein J. Org. Chem.*, 2014, **10**, 1197–1212.

28 E. Kaiser, R. L. Colescott, C. D. Bossinger and P. I. Cook, Color test for detection of free terminal amino groups in the solid-phase synthesis of peptides, *Anal. Biochem.*, 1970, **34**, 595–598.

29 R. Behrendt, P. White and J. Offer, Advances in Fmoc solid-phase peptide synthesis, *J. Pept. Sci.*, 2016, **22**, 4–27.

30 (a) J. R. Naglik, S. J. Challacombe and B. Hube, *Candida albicans* secreted aspartyl proteinases in virulence and pathogenesis, *Adv. Synth. Catal.*, 2003, **67**, 400–428; (b) M. Schaller, C. Borelli, H. C. Korting and B. Hube, Hydrolytic enzymes as virulence factors of *Candida albicans*, *Mycoses*, 2005, **48**, 365–377.

31 C. Borelli, E. Ruge, J. H. Lee, M. Schaller, A. Vogelsang, M. Monod, H. C. Korting, R. Huber and K. Maskos, X-ray structures of Sap1 and Sap5: structural comparison of the secreted aspartic proteinases from *Candida albicans*, *Proteins*, 2008, **72**, 1308–1319.

32 (a) H. M. Patel, M. Palkar and R. Karpoormath, Exploring MDR-TB inhibitory potential of 4-aminoquinazolines as mycobacterium tuberculosis N-acetylglucosamine-1-phosphate uridyltransferase (GlmUMTB) inhibitors, *Chem. Biodiversity*, 2020, **17**, e2000237; (b) H. Patel, K. Dhangar, Y. Sonawane, S. Surana, R. Karpoormath, N. Thapliyal, M. Shaikh, M. Noolvi and R. Jagtap, In search of selective 11  $\beta$ -HSD type 1 inhibitors without nephrotoxicity: an approach to resolve the metabolic syndrome by virtual based screening, *Arabian J. Chem.*, 2018, **11**, 221–232.

33 I. Ahmad, D. Kumar and H. Patel, Computational investigation of phytochemicals from *Withania somnifera* (Indian ginseng/ashwagandha) as plausible inhibitors of GluN<sub>2</sub>B-containing NMDA receptors, *J. Biomol. Struct. Dyn.*, 2022, **40**(17), 7991–8003.

34 I. Ahmad, M. Shaikh, S. Surana, A. Ghosh and H. Patel, p38 $\alpha$  MAP kinase inhibitors to overcome EGFR tertiary C797S point mutation associated with osimertinib in non-small cell lung cancer (NSCLC): emergence of fourth-generation EGFR inhibitor, *J. Biomol. Struct. Dyn.*, 2022, **40**(7), 3046–3059.

35 A. R. Zala, H. N. Naik, I. Ahmad, H. Patel, S. Jauhari and P. Kumari, Design and synthesis of novel 1, 2, 3-triazole linked hybrids: Molecular docking, MD simulation, and their antidiabetic efficacy as  $\alpha$ -Amylase inhibitors, *J. Mol. Struct.*, 2023, **1285**, 135493.

36 Y. O. Ayipo, I. Ahmad, W. Alananze, A. Lawal, H. Patel and M. N. Mordi, Computational modelling of potential Zn-sensitive non- $\beta$ -lactam inhibitors of imipenemase-1 (IMP-1), *J. Biomol. Struct. Dyn.*, 2022, **29**, 1–21.

37 N. C. Desai, A. S. Maheta, A. M. Jethawa, U. P. Pandit, I. Ahmad and H. Patel, Zeolite (Y-H)-based green synthesis, antimicrobial activity, and molecular docking studies of imidazole bearing oxydibenzene hybrid molecules, *J. Heterocycl. Chem.*, 2022, **59**(5), 879–889.



38 (a) D. Eisenberg, R. M. Weiss and T. C. Terwilliger, The helical hydrophobic moment: a measure of the amphiphilicity of a helix, *Nature*, 1982, **299**(5881), 371–374; (b) D. Eisenberg, E. Schwarz, M. Komaromy and R. Wall, Analysis of membrane and surface protein sequences with the hydrophobic moment plot, *J. Mol. Biol.*, 1984, **179**(1), 125–142.

39 (a) V. Pliska, M. Schmidt and J.-L. Fauchère, Partition coefficients of amino acids and hydrophobic parameters  $\pi$  of their sidechains as measured by thin-layer chromatography, *J. Chromatogr. A*, 1981, **216**, 79–92; (b) J.-L. Fauchère and V. Pliska, Hydrophobic parameters  $\pi$  of amino-acid side chains from the partitioning of N-acetyl-amino-acid amides, *Eur. J. Med. Chem.*, 1983, **18**(4), 7.

40 N. C. Desai, K. A. Jadeja, D. J. Jadeja, V. M. Khedkar, P. C. Jha and P. C. Design, synthesis, antimicrobial evaluation, and molecular docking study of some 4-thiazolidinone derivatives containing pyridine and quinazoline moiety, *Synth. Commun.*, 2021, **51**, 952–963.

41 B. Kowalska-Krochmal and R. Dudek-Wicher, The Minimum Inhibitory Concentration of Antibiotics: Methods, Interpretation, Clinical Relevance, *Pathogens*, 2021, **10**, 165.

42 J. H. Jorgensen and M. J. Ferraro, Antimicrobial susceptibility testing: a review of general principles and contemporary practices, *Clin. Infect. Dis.*, 2009, **49**, 1749–1755.

43 R. Hadianamrei, M. Tomeh, S. Brown, J. Wang and X. Zhao, Rationally designed short cationic  $\alpha$ -helical peptides with selective anticancer activity, *J. Colloid Interface Sci.*, 2021, **607**, 488–501.

44 Y. Huang, L. He, H. Jiang and Y. Chen, Role of Helicity on the Anticancer Mechanism of Action of Cationic-Helical Peptides, *Int. J. Mol. Sci.*, 2012, **13**, 6849–6862.

45 J. Hu, C. Chen, S. Zhang, X. Zhao, H. Xu, X. Zhao and J. Lu, Designed antimicrobial and antitumor peptides with high selectivity, *Biomacromolecules*, 2011, **12**, 3839–3843.

